

Properties Investigation of Sulfonated Poly(ether ether ketone)/Polyacrylonitrile Acid–Base Blend Membrane for Vanadium Redox Flow Battery Application

Zhaohua Li,^{†,‡} Wenjing Dai,^{†,‡} Lihong Yu,[§] Le Liu,[†] Jingyu Xi,^{*,†} Xinping Qiu,^{*,†,‡} and Liqun Chen^{†,‡}

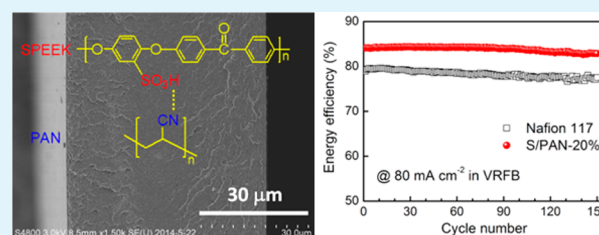
[†]Institute of Green Chemistry and Energy, Graduate School at Shenzhen, Tsinghua University, Shenzhen 518055, China

[‡]Key Lab of Organic Optoelectronics and Molecular Engineering, Department of Chemistry, Tsinghua University, Beijing 100084, China

[§]School of Applied Chemistry and Biological Technology, Shenzhen Polytechnic, Shenzhen 518055, China

ABSTRACT: Acid–base blend membrane prepared from sulfonated poly(ether ether ketone) (SPEEK) and polyacrylonitrile (PAN) was detailedly evaluated for vanadium redox flow battery (VRFB) application. SPEEK/PAN blend membrane exhibited dense and homogeneous cross-section morphology as scanning electron microscopy and energy-dispersive X-ray spectroscopy images show. The acid–base interaction of ionic cross-linking and hydrogen bonding between SPEEK and PAN could effectively reduce water uptake, swelling ratio, and vanadium ion permeability, and improve the performance and stability of blend membrane. Because of the good balance of proton conductivity and vanadium ion permeability, blend membrane with 20 wt % PAN (S/PAN-20%) showed higher Coulombic efficiency (96.2% vs 91.1%) and energy efficiency (83.5% vs 78.4%) than Nafion 117 membrane at current density of 80 mA cm⁻² when they were used in VRFB single cell. Besides, S/PAN-20% membrane kept a stable performance during 150 cycles at current density of 80 mA cm⁻² in the cycle life test. Hence the SPEEK/PAN acid–base blend membrane could be used as promising candidate for VRFB application.

KEYWORDS: vanadium redox flow battery, blend membrane, sulfonated poly(ether ether ketone), polyacrylonitrile, acid–base interaction



1. INTRODUCTION

Because of the need for large-scale energy storage systems to meet the requirements of increasing energy demand and power grid safety, vanadium redox flow battery (VRFB) has been extensively researched due to the features of high-energy efficiency, long cycle life, modular design, and flexible operation.^{1–4} The VRFB comprises VO₂⁺/VO²⁺ and V³⁺/V²⁺ redox couples in sulfuric acid as positive and negative electrolytes, carbon fabric materials as electrodes, and membranes as separators.^{5–8} As the key material of VRFB, numerous high-performance membranes have been reported.^{9–15} Nevertheless, the lack of appropriate low-cost membrane for long-term operation is a crucial issue for the advancement of VRFB.

Nafion membrane, state-of-the-art perfluorosulfonic polymer, is widely employed as the benchmark in VRFB owing to its high proton conductivity and excellent stability.^{16–18} To surmount the drawback of high vanadium ion permeability of Nafion membrane, modifications including composites and introduction of thin layer have been published with better VRFB performance than pristine Nafion membrane.^{19–23} However, the defect of essentially high cost of Nafion membrane would hinder the commercialization of VRFB.^{20,24} The anion-exchange membranes (AEMs)^{25,26} and porous

membranes²⁷ have been investigated for VRFB application recently. Because of the Donnan exclusion effect, the AEMs possess enormously low vanadium ion permeability and absorbed VO₂⁺ concentration, which could efficaciously reduce the degradation of AEMs. However, the dramatically low ionic conductivity would result in considerable low voltage efficiency and energy efficiency, which make AEMs unsuitable for high-power VRFB applications. The porous membranes are also unsuitable for large-scale VRFB applications owing to the heterogeneous and uncontrollable morphology, despite the high VRFB performance and good stability.

As one of the nonperfluorinated cation-exchange membranes (CEMs), the sulfonated polyaromatic membranes including sulfonated polysulfone,²⁸ sulfonated poly(phthalazinone ether ketone),²⁹ sulfonated fluorinated poly(arylene ether),³⁰ and sulfonated poly(ether ether ketone)^{31–34} have been widely researched for VRFB application. Owing to the features of low cost and easy preparation, the sulfonated poly(ether ether ketone) (SPEEK) membrane has attracted considerable attention.^{31–34} However, to achieve high proton conductivity,

Received: July 18, 2014

Accepted: October 15, 2014

Published: October 15, 2014

the high degree of sulfonation (DS) SPEEK membrane often causes high vanadium ion permeability and low VRFB performance and stability, which greatly hinder its further application in VRFB. Blending SPEEK with another polymer would be a facile way to obtain a membrane with comprehensive properties.^{35,36} Polyacrylonitrile (PAN) has been utilized in many fields due to its good mechanical property and chemical stability.^{37–39} The SPEEK and PAN, which are employed as acid polymer and base polymer, respectively, could be mixed together to get an acid–base blend membrane. The acid–base interaction of ionic cross-linking and hydrogen bonding between the sulfonic acid groups of SPEEK and the N-containing groups of PAN could reduce water uptake and vanadium ion permeability and then improve the performance of the blend membrane.^{40,41} Besides, PAN could reduce swelling ratio and improve mechanical properties of the blend membrane, leading to better stability for VRFB application.

Accordingly, SPEEK and PAN acid–base blend membranes were fabricated with various PAN mass ratios and investigated for vanadium redox flow battery application. The properties and VRFB performance of acid–base blend membranes were evaluated in detail.

2. EXPERIMENTAL SECTION

2.1. Materials. Poly(ether ether ketone) (PEEK 450G, Victrex) was purchased from local commercial agents. Polyacrylonitrile (PAN, average $M_w \approx 150\,000$) was purchased from Sigma-Aldrich Co. LLC. Nafion 117 membrane was purchased from DuPont Company. Other reagents were purchased from common commercial suppliers and used as received.

2.2. Membrane Preparation. Sulfonated poly(ether ether ketone) (SPEEK) with a high degree of sulfonation (DS) up to 0.79 was prepared via postsulfonation method.¹³ PAN was dissolved in N,N' -dimethylformamide at 60 °C for 2 h, and then SPEEK was added into the PAN solution to form an approximately 15 wt/vol % blend solution. The blend solution was cast onto a glass plate and then dried at 80 °C for 24 h. Afterward the membrane was peeled off by immersing the glass plate in deionized water, and then it soaked in 1 mol L⁻¹ H₂SO₄ solution for 24 h. Finally the membrane was washed with deionized water and then stored in deionized water at ambient temperature before it was used. The SPEEK/PAN acid–base blend membranes with various PAN mass ratios were denoted as S/PAN-X, where X was the PAN mass ratio. For example, S/PAN-20% membrane comprised 20 wt % PAN and 80 wt % SPEEK. The Nafion 117 membrane was pretreated and used as a benchmark.⁴²

2.3. Characterization. **2.3.1. Morphology and FTIR Spectra.** The cross-section morphology and energy-dispersive X-ray spectroscopy (EDX) element mapping of membrane was confirmed by scanning electron microscopy (SEM, S-4800, Hitachi). The cross-section sample was achieved by breaking membrane in liquid nitrogen and then coating it with gold. The Fourier transform infrared (FTIR) spectrum was recorded in the range of 4000–650 cm⁻¹ on an FTIR spectrometer (Nicolet 6700, Thermo Fisher Scientific Inc.) with 32 scans and 4 cm⁻¹ resolution at ambient temperature.

2.3.2. Physicochemical Properties, Mechanical Properties, VO²⁺ Permeability, and Ion Selectivity. The physicochemical properties and mechanical properties were investigated to get at least three parallel results, and the VO²⁺ permeability was conducted two times to get an average value. The physicochemical properties of water uptake, swelling ratio, ion-exchange capacity (IEC), and proton conductivity were measured as reported previously.¹³ The water uptake was defined as the ratio of absorbed water weight in wet membrane to dry membrane weight, while the swelling ratio was represented as the ratio of length change from wet to dry membrane. The IEC was examined by titration of H⁺ exchanged from membrane with 0.1 mol L⁻¹ NaOH solution and was described as the ratio of the consumed amount of

NaOH to dry membrane weight. The DS of SPEEK was calculated by the IEC result as reported previously.¹³ The proton conductivity was measured by two-probe electrochemical impedance spectroscopy (EIS) on a PARSTAT 2273 electrochemical station. The mechanical properties of air-dry membranes were detected on a MTS CMT-4204 electromechanical universal testing machine. The stretching dimensions of the sample were 25 mm × 4 mm, and the tensile speed was 5 mm min⁻¹. The VO²⁺ permeability was examined on a membrane-separated diffusion cell by filling VO²⁺ solution in left compartment and VO²⁺ blank solution in right compartment, followed by the standard procedures.⁴² The VO²⁺ concentration in right compartment was measured on a Leng Guang 752S UV–vis spectrometer, and the VO²⁺ permeability was calculated by the following equation:

$$V_R \frac{dC_R(t)}{dt} = A \frac{P}{L} (C_L - C_R(t)) \quad (1)$$

where P is VO²⁺ permeability, V_R is solution volume of right compartment, C_L and $C_R(t)$ are VO²⁺ concentration in left and right compartments, respectively, and A and L are area and thickness of membrane, respectively. The ion selectivity of membrane was an important indicator for VRFB and was defined as the ratio of proton conductivity to VO²⁺ permeability.

2.3.3. VRFB Single-Cell Test. The VRFB single-cell configuration was the same as reported previously⁴² as shown in Figure 1. The wet

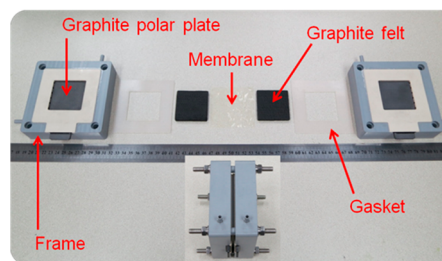


Figure 1. Configuration and assembly of VRFB single cell.

membrane thickness was 70–80 μm, and the geometry area of graphite felt was 25 cm². Two 50 mL solutions of 2.0 mol L⁻¹ vanadium ion ($C_{VO^{2+}}/C_{V^{3+}} = 1:1$) with 2.0 mol L⁻¹ free sulfuric acid (total 4.5 mol L⁻¹ SO₄²⁻) were applied as positive and negative electrolytes, respectively, and the electrolytes were cyclically pumped through the corresponding half-cells. The performance measurements were conducted on a Neware CT-3008W battery testing system, and the cutoff voltages were set at 1.65 and 0.8 V, respectively, to avoid the corrosion of graphite felts and graphite polar plates. The VRFB single cell was charged to 50% state of charge at current density of 60 mA cm⁻². Then the self-discharge test was begun and finished when the open circuit voltage was below 0.8 V. The charge–discharge test was performed at current densities from 40 to 200 mA cm⁻². Four cycles were done at each current density, and the average efficiency values were obtained. The cycle life test was conducted at current density of 80 mA cm⁻². The Coulombic efficiency (CE), voltage efficiency (VE), and energy efficiency (EE) were calculated by the following equations:

$$CE(\%) = \frac{\int I_d dt}{\int I_c dt} \times 100 \quad (2)$$

$$EE(\%) = \frac{\int V_d I_d dt}{\int V_c I_c dt} \times 100 \quad (3)$$

$$VE(\%) = \frac{EE}{CE} \times 100 \quad (4)$$

where I_c and I_d are the charge current and discharge current, respectively, and V_c and V_d are the charge voltage and discharge voltage, respectively.

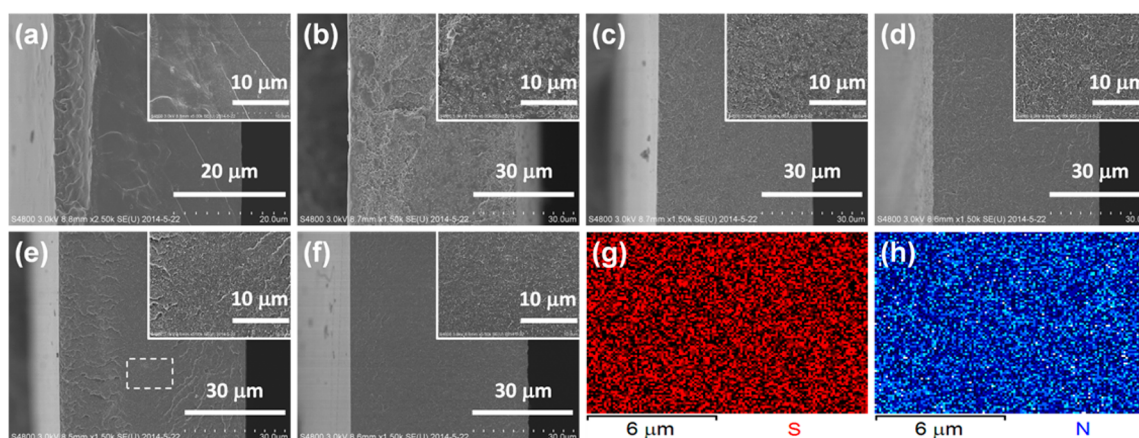


Figure 2. Cross-section SEM images of membranes: (a) SPEEK, (b) S/PAN-5%, (c) S/PAN-10%, (d) S/PAN-15%, (e) S/PAN-20%, (f) S/PAN-25%. (insets) The corresponding high-resolution SEM images. EDX element mapping of S/PAN-20% membrane: (g) element S and (h) element N.

2.3.4. Chemical Stability Test. The membrane chemical stability was investigated with both low and high concentration V(V) solutions.^{43–45} Two sample membranes were soaked in 30 mL of 0.1 mol L⁻¹ V(V) with 3.0 mol L⁻¹ free sulfuric acid and in 30 mL of 1.5 mol L⁻¹ V(V) with 3.0 mol L⁻¹ free sulfuric acid, respectively. Various mixing ratios of V(IV)/V(V) solutions (total vanadium concentration was 0.1 mol L⁻¹) were prepared, and the absorbance of mixtures was measured with UV–vis spectrometer (752S, Leng Guang Tech.) at 760 nm to make a standard curve. The concentration of V(IV) ions in the soaking solutions was determined by the UV–vis spectrometer. The average data was obtained from two sets of sample membranes. The weight loss and reduction of V(V) to V(IV) of sample membrane were calculated by following equations:

$$\text{weight loss(\%)} = \frac{W_0 - W}{W_0} \times 100 \quad (5)$$

$$\text{reduction of V(V) to V(IV)(\%)} = \frac{C_{V(IV)}}{C_{V(V)}} \times 100 \quad (6)$$

where W_0 and W are the weight of dry sample membrane before and after soaking in V(V) solution for two weeks, $C_{V(IV)}$ is the concentration of the V(IV) reduced from V(V) solution after two weeks, and $C_{V(V)}$ is the concentration of initial V(V) solution.

3. RESULTS AND DISCUSSION

3.1. Morphology and FTIR Spectra. The dense and homogeneous cross-section morphology of SPEEK and SPEEK/PAN acid–base blend membranes were observed in Figure 2 a–f, demonstrating the good compatibility of two components. The high-resolution SEM images (insets of Figure 2b–f) showed that the cross-section morphology of blend membranes was getting smoother with the increases of PAN mass ratio, suggesting the increasing of acid–base interaction between SPEEK and PAN. Moreover, the region encircled by white dash line in Figure 2e was investigated by EDX, and the EDX element mapping of S/PAN-20% membrane was illustrated in Figure 2g,h. The element S (red color points in Figure 2g), representing SPEEK, and element F (blue color points in Figure 2h), representing PAN, were uniformly dispersed, indicating the homogeneous morphology of blend membranes.

Similar FTIR spectra of SPEEK and SPEEK/PAN blend membranes were represented in Figure 3. Typical absorption peaks of SPEEK could be found including carbonyl stretching at 1640 cm⁻¹, asymmetric and symmetric stretching of O=S=O at 1251 and 1076 cm⁻¹, respectively, and asymmetric

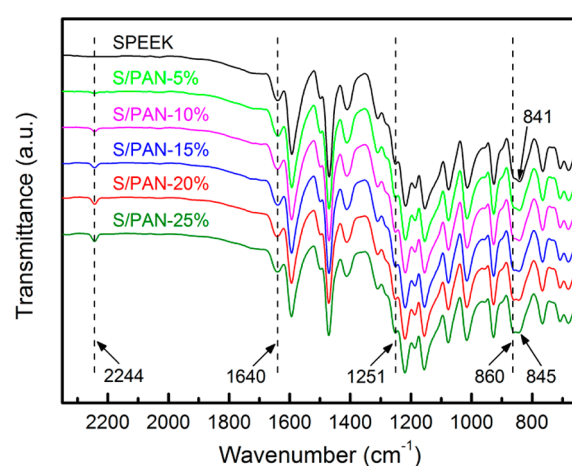


Figure 3. FTIR spectra of SPEEK and SPEEK/PAN blend membranes.

stretching of diphenyl ether groups at 1218 cm⁻¹.^{46–48} The peak at 2244 cm⁻¹ was attributed to the C≡N stretching of PAN,^{47,48} and the peak intensity increased with the increasing of PAN mass ratio. The peak at 861 cm⁻¹ was assigned to the out-of-plane C–H bending of the isolated hydrogen in the 1,2,4-trisubstituted phenyl ring of SPEEK. The increasing of peak intensity at 861 cm⁻¹ could be due to the increasing of acid–base interaction comprised of ionic cross-linking and hydrogen bonding between SPEEK and PAN as described in Figure 4.^{40,41} The peak shift from 841 cm⁻¹ (out-of-plane bending of two hydrogen atoms of 1,4-disubstituted phenyl ring) to 845 cm⁻¹ also could be assigned to the influence of the acid–base interaction.

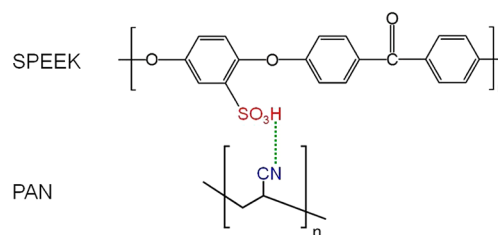


Figure 4. Schematic of acid–base interaction between SPEEK and PAN.

3.2. Physicochemical Properties, Mechanical Properties, VO^{2+} Permeability, and Ion Selectivity. The physicochemical properties of various membranes comprised water uptake, swelling ratio, ion exchange capacity (IEC), and proton conductivity as shown in Figure 5, and the

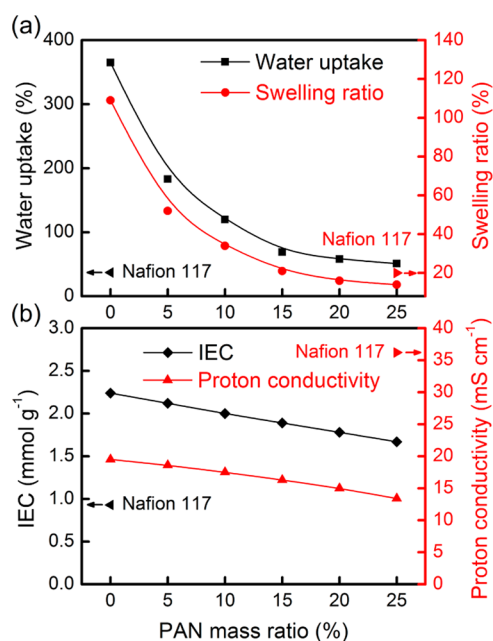


Figure 5. Physicochemical properties of Nafion 117, SPEEK, and SPEEK/PAN blend membranes: (a) water uptake and swelling ratio; (b) ion-exchange capacity and proton conductivity.

corresponding data are listed in Table 1. The extremely high water uptake and swelling ratio of SPEEK membrane were disadvantageous for VRFB as shown in Figure 5a.⁶ The incorporation of PAN obviously reduced water uptake and swelling ratio of SPEEK/PAN blend membranes, which could be owing to the stronger acid–base interaction (see Figure 4) and the decreasing of SPEEK component with the increasing PAN mass ratio. The decreasing of water uptake of blend membranes would cause lower vanadium ion permeability and higher VRFB performance compared with SPEEK membrane.¹⁶ The lower swelling ratio of blend membranes compared with SPEEK membrane would result in higher mechanical property and better stability and then lead to more stable VRFB performance and slower capacity fade.^{14,33} The IEC and proton conductivity of various membranes are shown in Figure 5b. The IEC of blend membranes decreased the same proportion with the decreasing of SPEEK component, demonstrating that the acid–base interaction had no hindrance during ion-exchange

process. Proton conductivity was mainly affected by water uptake and IEC.^{49–51} Therefore, the proton conductivity of blend membranes decreased with the decreasing of water uptake and IEC as shown in Figure 5b. Generally, higher proton conductivity was beneficial for VRFB. However, the vanadium ion permeability and membrane stability of SPEEK-based membrane were mainly affected by the high water uptake. Therefore, the optimized blend membrane with the good balance of proton conductivity and vanadium ion permeability would lead to better and more stable VRFB performance.

The tensile curves and mechanical properties of various membranes were illustrated in Figure 6. As shown in Figure 6a,

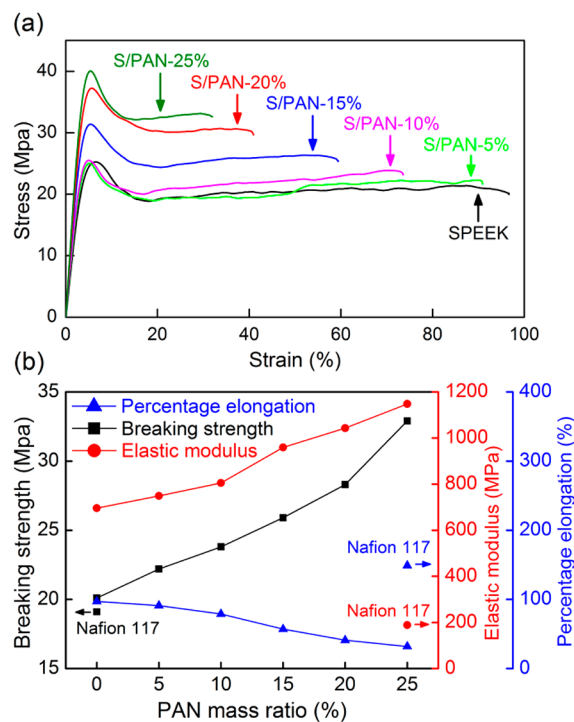


Figure 6. Tensile curves (a) and mechanical properties (b) of Nafion 117, SPEEK, and SPEEK/PAN blend membranes.

the stress and strain of blend membranes increased and decreased, respectively, with the increasing of PAN mass ratio, which was due to the acid–base interaction and the good mechanical property of PAN. The yield stress of S/PAN-15%, S/PAN-20%, and S/PAN-25% membranes exhibited obvious increase, revealing better mechanical properties than other membranes. The breaking strength, elastic modulus, and percentage elongation of various membranes are shown in

Table 1. Data of Physicochemical Properties, Mechanical Properties, VO^{2+} Permeability, and Ion Selectivity

membrane	water uptake (%)	swelling ratio (%)	IEC (mmol g ⁻¹)	proton conductivity (mS cm ⁻¹)	breaking strength (MPa)	elastic modulus (MPa)	percentage elongation (%)	VO^{2+} permeability (10 ⁻⁷ cm ² min ⁻¹)	ion selectivity (10 ³ S min cm ⁻³)
Nafion 117	37 ± 1	20 ± 1	0.93 ± 0.01	36.2 ± 1.0	19.1 ± 0.3	189 ± 7	149 ± 3	37.7 ± 0.4	9.6 ± 0.4
SPEEK	365 ± 18	109 ± 5	2.24 ± 0.01	19.5 ± 0.3	20.1 ± 0.3	696 ± 15	97 ± 2	76.6 ± 2.6	2.6 ± 0.2
S/PAN-5%	183 ± 7	52 ± 2	2.12 ± 0.01	18.6 ± 0.4	22.2 ± 0.4	749 ± 19	91 ± 3	48.4 ± 0.8	3.8 ± 0.2
S/PAN-10%	120 ± 4	34 ± 2	2.00 ± 0.01	17.5 ± 0.3	23.8 ± 0.5	805 ± 20	79 ± 4	29.9 ± 0.2	5.9 ± 0.2
S/PAN-15%	69 ± 2	21 ± 1	1.89 ± 0.01	16.3 ± 0.4	25.9 ± 0.7	959 ± 21	57 ± 2	17.8 ± 0.1	9.2 ± 0.3
S/PAN-20%	58 ± 1	16 ± 1	1.78 ± 0.01	15.0 ± 0.3	28.3 ± 1.1	1043 ± 29	41 ± 1	11.3 ± 0.1	13.3 ± 0.4
S/PAN-25%	51 ± 1	14 ± 1	1.67 ± 0.01	13.4 ± 0.2	32.9 ± 1.5	1148 ± 25	32 ± 1	7.7 ± 0.1	17.4 ± 0.5

Figure 6b and Table 1. Because of the structural differences between the SPEEK and Nafion 117 membranes,^{49,50} the SPEEK membrane possessed higher rigidity than that of the Nafion 117 membrane. Therefore, higher breaking strength, higher elastic modulus, and lower percentage elongation of SPEEK membrane could be observed. The increasing of acid–base interaction and PAN component further improved the mechanical properties of blend membranes, leading to the increasing of breaking strength and elastic modulus and the decreasing of percentage elongation. Although the percentage elongation of blend membranes was lower than that of the Nafion 117 membrane, the blend membranes were flexible enough for the VRFB single-cell test.

The schematic illustration of membrane-separated diffusion cell, VO^{2+} permeability, and ion selectivity of various membranes are shown in Figure 7. The data are listed in

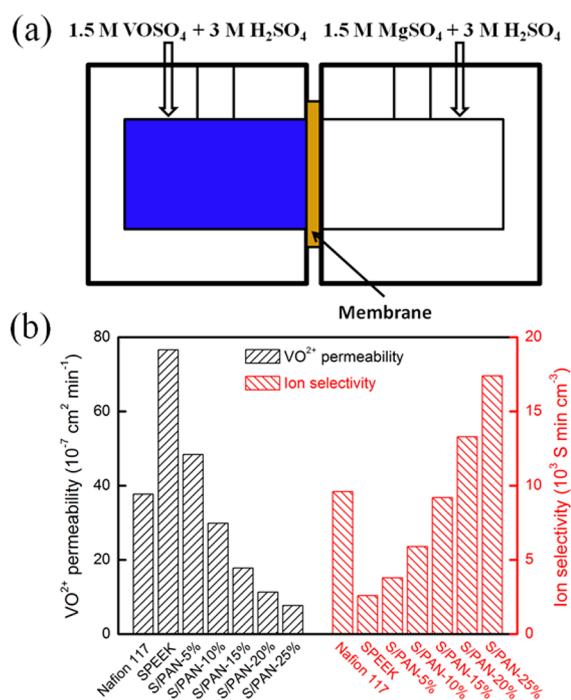


Figure 7. VO^{2+} permeability test device and results: (a) schematic illustration of membrane-separated diffusion cell; (b) VO^{2+} permeability and ion selectivity of various membranes.

Table 1. The VO^{2+} permeability of blend membranes decreased with the increasing of PAN mass ratio. The acid–base interaction would reduce water uptake and hydrophilic domains of blend membranes, leading to lower cross-mixing of vanadium ions and higher VRFB Coulombic efficiency. As a key parameter of VRFB, the ion selectivity could evaluate the balance of proton conductivity and vanadium ion permeability. Normally higher ion selectivity represented better VRFB performance.^{13,33} The ion selectivity of S/PAN-15%, S/PAN-20%, and S/PAN-25% membranes were close to or higher than that of the Nafion 117 membrane, suggesting that these membranes were better than other membranes in this work for VRFB application.

3.3. VRFB Single-Cell Performance. To confirm the good trends of properties of SPEEK/PAN blend membranes, the self-discharge test of various membranes was conducted. The self-discharge test was begun at 50% state of charge and finished when the open circuit voltage was below 0.8 V. As

shown in Figure 8, the self-discharge time of various membranes were consistent with the VO^{2+} permeability and

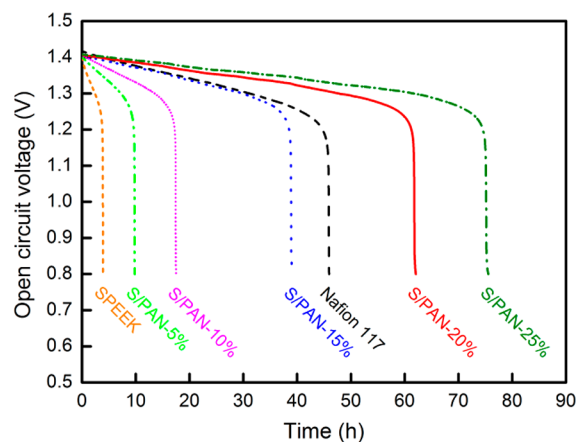


Figure 8. Self-discharge curves of Nafion 117, SPEEK, and SPEEK/PAN blend membranes.

ion selectivity results. The incorporation of PAN effectively reduced the cross-mixing of vanadium ions, causing a longer self-discharge time than that of the SPEEK membrane. The self-discharge times of S/PAN-15%, S/PAN-20%, and S/PAN-25% membranes were close to or higher than that of the Nafion 117 membrane, indicating better properties for further test. Because of the acid–base interaction between SPEEK and PAN, the blend membranes exhibited good trends of physicochemical properties, mechanical properties, VO^{2+} permeability, ion selectivity, and self-discharge time with the increase of PAN mass ratio. Furthermore, the S/PAN-15%, S/PAN-20%, and S/PAN-25% membranes were selected to perform further investigation owing to the similar or better properties compared with Nafion 117 membrane.

The charge–discharge test was conducted at constant current densities from 40 to 200 mA cm^{-2} , and the charge–discharge curves of VRFBs assembled with various membranes at constant current densities of 40, 80, 120, 160, and 200 mA cm^{-2} were represented in Figure 9a–e. The capacities of all membranes decreased with the increasing current density. Because of the higher IR drop at higher current density, higher charge voltage and lower discharge voltage were observed, leading to the decreasing of capacities when the amount of electrolyte was fixed in this test. The capacities of SPEEK/PAN blend membranes were higher than that of Nafion 117 membrane at all current densities, revealing the higher utilization of electrolyte, which was beneficial for reducing the actual amount of electrolyte. Besides, higher capacities of blend membranes also demonstrated higher VRFB single-cell performance. The S/PAN-20% membrane exhibited highest capacities within these membranes, which could be attributed to its good balance of proton conductivity and vanadium ion permeability. The capacities of S/PAN-15% membrane were fewer than S/PAN-20% membrane, which could be assigned to the higher vanadium ion permeability and higher cross-mixing of vanadium ions. The S/PAN-25% membrane also possessed fewer capacities than S/PAN-20% membrane, although the ion selectivity of S/PAN-25% membrane was highest. This was due to the lower proton conductivity of S/PAN-25% membrane, resulting in higher ohmic polarization and fewer capacities. As shown in Figure 9f, the discharge energy and average discharge

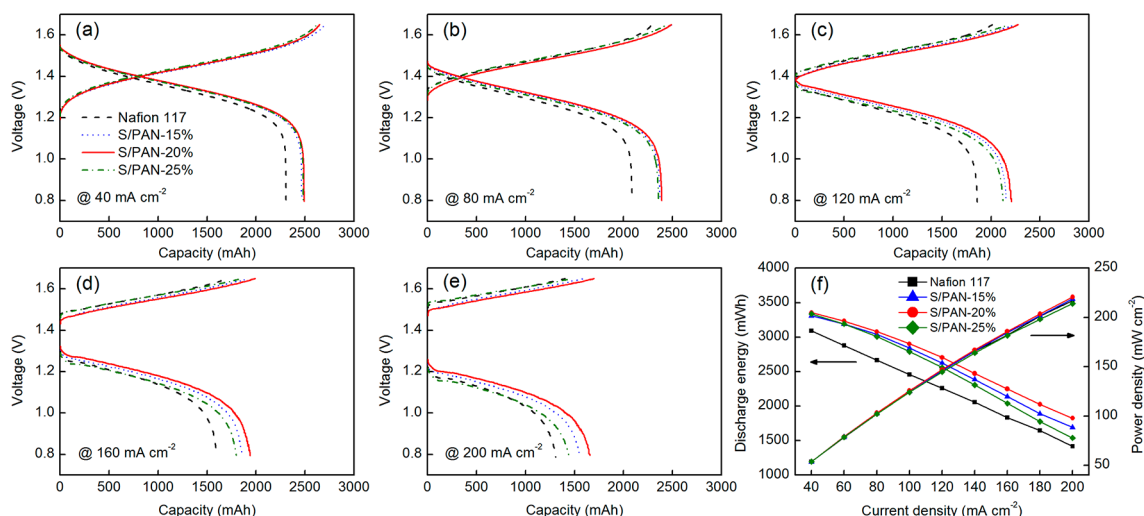


Figure 9. Charge–discharge curves at constant current densities of (a) 40 mA cm⁻², (b) 80 mA cm⁻², (c) 120 mA cm⁻², (d) 160 mA cm⁻², (e) 200 mA cm⁻²; and (f) discharge energy and average discharge power density of VRFBs assembled with various membranes.

power density maintained the same order as shown in the charge–discharge curves, where the S/PAN-20% membrane exhibited highest values within these membranes at all current densities.

The charge–discharge performance of Coulombic efficiency (CE), voltage efficiency (VE), and energy efficiency (EE) of VRFBs assembled with various membranes were illustrated in Figure 10. The deviation of efficiency value was less than 0.5%

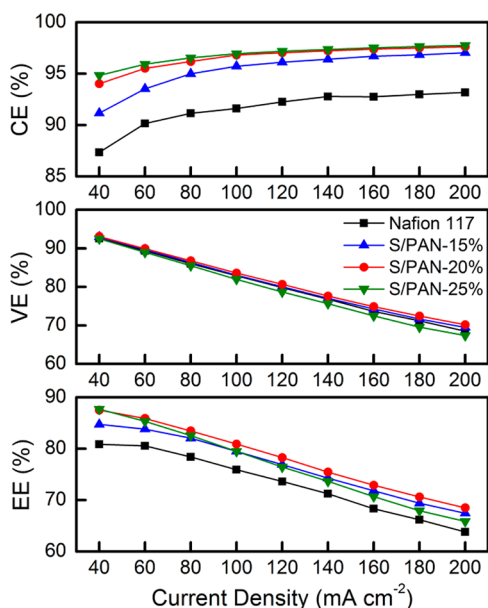


Figure 10. Coulombic efficiency (CE), voltage efficiency (VE), and energy efficiency (EE) of VRFBs assembled with Nafion 117, S/PAN-15%, S/PAN-20%, and S/PAN-25% membranes at constant current densities from 40 to 200 mA cm⁻².

in the charge–discharge test and cycle life test. Because of the identical configuration of VRFB single cell except membrane, CE was dominantly affected by the cross-mixing of vanadium ions.^{25,42} Therefore, the blend membranes exhibited higher CE than Nafion 117 membrane according to the VO²⁺ permeability results, and the order of CE was S/PAN-25%, S/PAN-20%, S/PAN-15%, and Nafion 117 membranes. The increasing of CE

with the increasing of current density could be assigned to shorter charge–discharge time at higher current density, resulting in lower cross-mixing of vanadium ions and capacity loss.¹⁴ The VE rank was S/PAN-20%, S/PAN-15%, Nafion 117, and S/PAN-25% membranes. The lowest VE of S/PAN-25% membrane could be attributed to the lowest proton conductivity and highest IR drop. The gradual decreasing of VE with the increase of current density could be assigned to the increase of ohmic polarization. EE was an important indicator of energy loss during the charge–discharge process and often employed in the energy storage system.³³ The order of EE was the same as shown in the charge–discharge curves, where the blend membranes exhibited higher EE than Nafion 117 membrane. Because of the lower proton conductivity, the EE decreasing of S/PAN-25% membrane was also larger than other membranes, causing lower EE than S/PAN-15% membrane above current density of 100 mA cm⁻². Owing to the good balance of proton conductivity and vanadium ion permeability accompanied by suitable proton conductivity, S/PAN-20% membrane showed highest EE within these membranes at all current densities. The VRFB single-cell performance of S/PAN-20% membrane showed higher CE (96.2% vs 91.1%) and EE (83.5% vs 78.4%) than Nafion 117 membrane at current density of 80 mA cm⁻², revealing the advancement for VRFB application.

The cycle life test of VRFBs assembled with Nafion 117 and S/PAN-20% membranes were performed at constant current density of 80 mA cm⁻² to investigate the membrane stability in actual VRFB operation. The cycle performances of CE, EE, and discharge capacity retention were illustrated in Figure 11. The CE and EE of Nafion 117 and S/PAN-20% membranes kept stable during 150 cycles, indicating that both membranes could effectively resist the degradation under the severe VRFB operation. Besides, the CE and EE values of S/PAN-20% membrane were consistent with the results of charge–discharge test (see Figure 10), demonstrating the good reproducibility of SPEEK/PAN acid–base blend membranes. The discharge capacity fade of S/PAN-20% membrane was slower than Nafion 117 membrane. After 150 cycles, the discharge capacity retention of Nafion 117 and S/PAN-20% membranes were 46% and 34%, respectively, indicating the good stability of S/PAN-20% membrane.

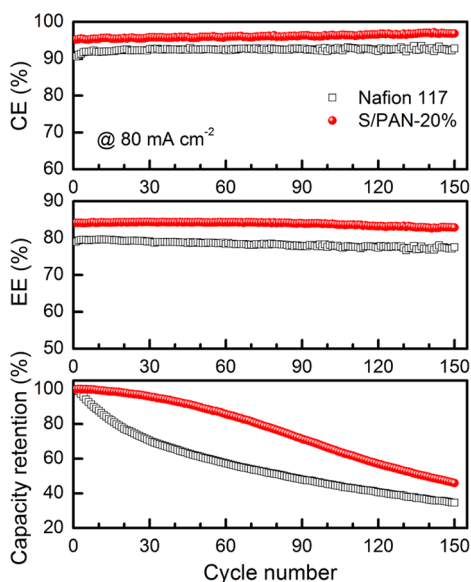


Figure 11. Coulombic efficiency (CE), energy efficiency (EE), and discharge capacity retention of VRFBs assembled with Nafion 117 and S/PAN-20% membranes at constant current density of 80 mA cm^{-2} .

The charge–discharge curves of Nafion 117 and S/PAN-20% membranes at different cycles in the cycle life test were illustrated in Figure 12. The capacities of both membranes decreased with the increase of cycle number, while the higher charge voltage and lower discharge voltage could be observed.

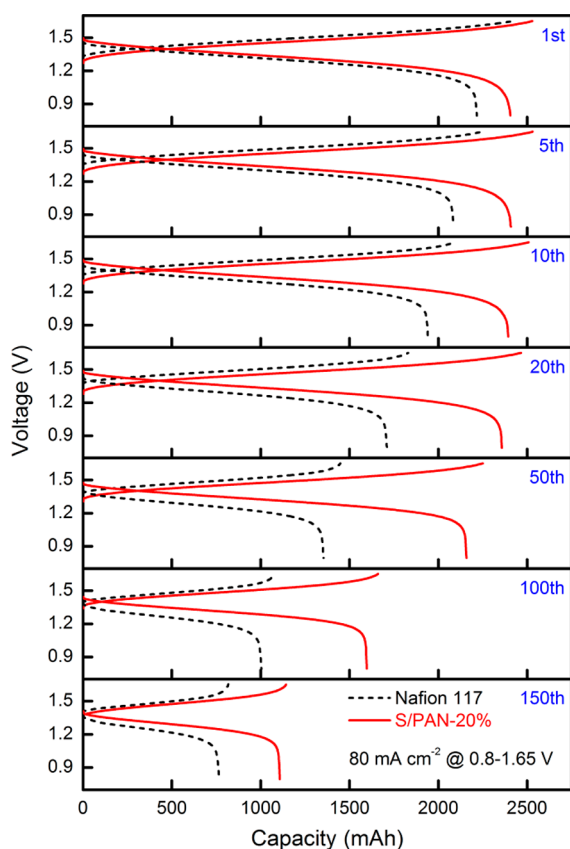


Figure 12. Charge–discharge curves of Nafion 117 and S/PAN-20% membranes in the cycle life. The number in the figure is the specific cycle number.

The volume and vanadium ion concentration of electrolytes would be imbalanced due to the imbalanced migration of vanadium ions, hydrogen ions, and water.⁵ With the increase of cycle number, the imbalance of electrolytes would be larger, leading to higher state of charge of electrolyte in one side of VRFB single cell. Therefore, higher polarization and lower capacity was observed. The capacity difference between Nafion 117 and S/PAN-20% membranes increased with the increasing of cycle number until 50th cycle. The smaller capacity difference after 50 cycles may be due to the swelling behavior of S/PAN-20 membrane, which could lead to larger cross-mixing of vanadium ions and faster capacity fade than the foregoing cycles. Nevertheless, the cycle performance of S/PAN-20% membrane was still better than Nafion 117 membrane. The SPEEK/PAN acid–base blend membranes possessed higher, stable CE and EE and slower discharge capacity fade, indicating the good applicability of SPEEK/PAN blend membranes and good prospect for VRFB applications.

3.4. Chemical Stability. The chemical stability of Nafion 117 and S/PAN-20% membranes were further investigated by soaking membranes in both low and high concentration (0.1 and 1.5 mol L^{-1}) V(V) solutions for two weeks.^{43–45} The results are listed in Table 2. The chemical degradation of

Table 2. Chemical Stability Results of Nafion 117 and S/PAN-20% Membranes by Soaking in V(V) Solutions for Two Weeks

membrane	weight loss (%)		reduction of V(V) to V(IV) (%)	
	0.1 mol L^{-1} (V)	1.5 mol L^{-1} (V)	0.1 mol L^{-1} (V)	1.5 mol L^{-1} (V)
Nafion 117	0.1	0.4 ± 0.1	0.0	0.1
S/PAN-20%	0.5 ± 0.1	4.0 ± 0.3	0.3	2.9 ± 0.2

membrane could be due to the degradation of membrane backbone.⁴⁵ Hence the V(IV) reduced from V(V) indicates the stability of membrane. The Nafion 117 membrane showed extremely low weight loss and V(IV) reduced from V(V), revealing the high chemical stability in both low and high concentration V(V) solutions. The S/PAN-20% membrane also exhibited high chemical stability as shown in Table 2. The V(IV) reduced from V(V) was only 2.9% after soaking in 1.5 mol L^{-1} V(V) solution for two weeks, suggesting the good chemical stability and long lifetime of S/PAN-20% membrane.

4. CONCLUSIONS

SPEEK/PAN acid–base blend membranes with various PAN mass ratios (5%, 10%, 15%, 20%, and 25%) were prepared and investigated in detail in VRFB. SEM and EDX results indicated that blend membranes maintained dense and homogeneous cross-section morphology. The acid–base interaction of ionic cross-linking and hydrogen bonding between SPEEK and PAN was proposed and confirmed by FTIR spectra. The good trends of physicochemical properties, mechanical properties, VO^{2+} permeability, ion selectivity, and self-discharge time with the increase of PAN mass ratio possessed by blend membranes also supported the existence of acid–base interaction. The S/PAN-15%, S/PAN-20%, and S/PAN-25% membranes were chosen to perform further VRFB single-cell test. Because of the good balance of proton conductivity and vanadium ion permeability accompanied by suitable proton conductivity, S/PAN-20%

membrane showed higher VRFB performance of CE (96.2% vs 91.1%) and EE (83.5% vs 78.4%) than Nafion 117 membrane at current density of 80 mA cm⁻². Furthermore, S/PAN-20% membrane exhibited identical, stable CE and EE during 150 cycles in the cycle life test, and the discharge capacity retention (46% vs 34%) was higher than Nafion 117 membrane after 150 cycles. Therefore, the low-cost SPEEK/PAN acid–base blend membranes showed good prospect of substituting Nafion membrane for VRFB application.

AUTHOR INFORMATION

Corresponding Authors

*E-mail: xijingyu@gmail.com. (J.X.)

*E-mail: qiuxp@tsinghua.edu.cn. (X.Q.)

Notes

The authors declare no competing financial interest.

ACKNOWLEDGMENTS

This work was supported by the National Basic Research Program of China (2009CB220105, 2013CB934000), National Natural Science Foundation of China (21273129, 20973099), Shenzhen Science Fund for Distinguished Young Scholars (JC201104210149A), and Shenzhen Basic Research Project (CXZZ20130322164607310, JCYJ20130402145002403, and JCYJ20120830152316442). The authors thank Miss B. Yin and Prof. L. Wang from Shenzhen University for the FTIR and mechanical properties measurements.

REFERENCES

- (1) Dunn, B.; Kamath, H.; Tarascon, J. M. Electrical Energy Storage for the Grid: A Battery of Choices. *Science* **2011**, *334*, 928–935.
- (2) Yang, Z.; Zhang, J.; Kintner-Meyer, M. C. W.; Lu, X.; Choi, D.; Lemmon, J. P.; Liu, J. Electrochemical Energy Storage for Green Grid. *Chem. Rev.* **2011**, *111*, 3577–3613.
- (3) Cheng, F.; Liang, J.; Tao, Z.; Chen, J. Functional Materials for Rechargeable Batteries. *Adv. Mater.* **2011**, *23*, 1695–1715.
- (4) Armaroli, N.; Balzani, V. Towards an Electricity-Powered World. *Energy Environ. Sci.* **2011**, *4*, 3193–3222.
- (5) Parasuraman, A.; Lim, T. M.; Menictas, C.; Skyllas-Kazacos, M. Review of Material Research and Development for Vanadium Redox Flow Battery Applications. *Electrochim. Acta* **2013**, *101*, 27–40.
- (6) Ding, C.; Zhang, H.; Li, X.; Liu, T.; Xing, F. Vanadium Flow Battery for Energy Storage: Prospects and Challenges. *J. Phys. Chem. Lett.* **2013**, *4*, 1281–1294.
- (7) Liu, L.; Xi, J.; Wu, Z.; Zhang, W.; Zhou, H.; Li, W.; Qiu, X. State of Charge Monitoring for Vanadium Redox Flow Batteries by the Transmission Spectra of V(IV)/V(V) Electrolytes. *J. Appl. Electrochem.* **2012**, *42*, 1025–1031.
- (8) Zhang, W.; Xi, J.; Li, Z.; Zhou, H.; Liu, L.; Wu, Z.; Qiu, X. Electrochemical Activation of Graphite Felt Electrode for VO²⁺/VO₂⁺ Redox Couple Application. *Electrochim. Acta* **2013**, *89*, 429–435.
- (9) Teng, X.; Zhao, Y.; Xi, J.; Wu, Z.; Qiu, X.; Chen, L. Nafion/Organic Silica Hybrid Membrane for Vanadium Redox Flow Battery. *Acta Chim. Sin.* **2009**, *67*, 471–476.
- (10) Teng, X.; Zhao, Y.; Xi, J.; Wu, Z.; Qiu, X.; Chen, L. Nafion/Organic Silica Modified TiO₂ Composite Membrane for Vanadium Redox Flow Battery via in situ Sol–Gel Reactions. *J. Membr. Sci.* **2009**, *341*, 149–154.
- (11) Kim, S.; Yan, J.; Schwenzler, B.; Zhang, J.; Li, L.; Liu, J.; Yang, Z.; Hickner, M. A. Cycling Performance and Efficiency of Sulfonated Poly(Sulfone) Membranes in Vanadium Redox Flow Batteries. *Electrochem. Commun.* **2010**, *12*, 1650–1653.
- (12) Teng, X.; Dai, J.; Su, J.; Zhu, Y.; Liu, H.; Song, Z. A High Performance Polytetrafluoroethylene/Nafion Composite Membrane for Vanadium Redox Flow Battery Application. *J. Power Sources* **2013**, *240*, 131–139.
- (13) Li, Z.; Xi, J.; Zhou, H.; Liu, L.; Wu, Z.; Qiu, X.; Chen, L. Preparation and Characterization of Sulfonated Poly(Ether Ether Ketone)/Poly(Vinylidene Fluoride) Blend Membrane for Vanadium Redox Flow Battery Application. *J. Power Sources* **2013**, *237*, 132–140.
- (14) Chen, D.; Hickner, M. A.; Agar, E.; Kumbur, E. C. Optimized Anion Exchange Membranes for Vanadium Redox Flow Batteries. *ACS Appl. Mater. Interfaces* **2013**, *5*, 7559–7566.
- (15) Xu, Z.; Michos, I.; Wang, X.; Yang, R.; Gu, X.; Dong, J. A Zeolite Ion Exchange Membrane for Redox Flow Batteries. *Chem. Commun.* **2014**, *50*, 2416–2419.
- (16) Li, X.; Zhang, H.; Mai, Z.; Zhang, H.; Vankelecom, I. Ion Exchange Membranes for Vanadium Redox Flow Battery (VRB) Applications. *Energy Environ. Sci.* **2011**, *4*, 1147–1160.
- (17) Schwenzler, B.; Zhang, J.; Kim, S.; Li, L.; Liu, J.; Yang, Z. Membrane Development for Vanadium Redox Flow Batteries. *ChemSusChem* **2011**, *4*, 1388–1406.
- (18) Prifti, H.; Parasuraman, A.; Winardi, S.; Lim, T. M.; Skyllas-Kazacos, M. Membranes for Redox Flow Battery Applications. *Membranes* **2012**, *2*, 275–306.
- (19) Xi, J.; Wu, Z.; Qiu, X.; Chen, L. Nafion/SiO₂ Hybrid Membrane for Vanadium Redox Flow Battery. *J. Power Sources* **2007**, *166*, 531–536.
- (20) Xi, J.; Wu, Z.; Teng, X.; Zhao, Y.; Chen, L.; Qiu, X. Self-Assembled Polyelectrolyte Multilayer Modified Nafion Membrane with Suppressed Vanadium Ion Crossover for Vanadium Redox Flow Batteries. *J. Mater. Chem.* **2008**, *18*, 1232–1238.
- (21) Wang, N.; Peng, S.; Lu, D.; Liu, S.; Liu, Y.; Huang, K. Nafion/TiO₂ Hybrid Membrane Fabricated via Hydrothermal Method for Vanadium Redox Battery. *J. Solid State Electrochem.* **2012**, *16*, 1577–1584.
- (22) Teng, X.; Zhao, Y.; Xi, J.; Wu, Z.; Qiu, X.; Chen, L. Nafion/Organically Modified Silicate Hybrids Membrane for Vanadium Redox Flow Battery. *J. Power Sources* **2009**, *189*, 1240–1246.
- (23) Lu, S.; Wu, C.; Liang, D.; Tan, Q.; Xiang, Y. Layer-by-layer Self-Assembly of Nafion-[CS-PWA] Composite Membranes with Suppressed Vanadium Ion Crossover for Vanadium Redox Flow Battery Applications. *RSC Adv.* **2014**, *4*, 24831–24837.
- (24) Chalamala, B. R.; Soundappan, T.; Fisher, G. R.; Anstey, M. R.; Viswanathan, V. V.; Perry, M. L. Redox Flow Batteries: An Engineering Perspective. *Proc. IEEE* **2014**, *102*, 976–999.
- (25) Chen, D.; Hickner, M. A.; Agar, E.; Kumbur, E. C. Selective Anion Exchange Membranes for High Coulombic Efficiency Vanadium Redox Flow Batteries. *Electrochem. Commun.* **2013**, *26*, 37–40.
- (26) Jung, M. J.; Parrondo, J.; Arges, C. G.; Ramani, V. Polysulfone-Based Anion Exchange Membranes Demonstrate Excellent Chemical Stability and Performance for the All-Vanadium Redox Flow Battery. *J. Mater. Chem. A* **2013**, *1*, 10458–10464.
- (27) Li, Y.; Zhang, H.; Li, X.; Zhang, H.; Wei, W. Porous Poly (Ether Sulfone) Membranes with Tunable Morphology: Fabrication and Their Application for Vanadium Flow Battery. *J. Power Sources* **2013**, *233*, 202–208.
- (28) Chen, D.; Hickner, M. A. V⁵⁺ Degradation of Sulfonated Radel Membranes for Vanadium Redox Flow Batteries. *Phys. Chem. Chem. Phys.* **2013**, *15*, 11299–11305.
- (29) Wang, N.; Yu, J.; Zhou, Z.; Fang, D.; Liu, S.; Liu, Y. SPPEK/TPA Composite Membrane as A Separator of Vanadium Redox Flow Battery. *J. Membr. Sci.* **2013**, *437*, 114–121.
- (30) Chen, D.; Kim, S.; Sprenkle, V.; Hickner, M. A. Composite Blend Polymer Membranes with Increased Proton Selectivity and Lifetime for Vanadium Redox Flow Batteries. *J. Power Sources* **2013**, *231*, 301–306.
- (31) Wang, Y.; Wang, S.; Xiao, M.; Han, D.; Hickner, M. A.; Meng, Y. Layer-by-Layer Self-Assembly of PDDA/PSS-SPPEK Composite Membrane with Low Vanadium Permeability for Vanadium Redox Flow Battery. *RSC Adv.* **2013**, *3*, 15467–15474.
- (32) Dai, W.; Yu, L.; Li, Z.; Yan, J.; Liu, L.; Xi, J.; Qiu, X. Sulfonated Poly(Ether Ether Ketone)/Graphene Composite Membrane for Vanadium Redox Flow Battery. *Electrochim. Acta* **2014**, *132*, 200–207.

(33) Chen, D.; Li, X. Sulfonated Poly(Ether Ether Ketone) Membranes Containing Pendent Carboxylic Acid Groups and Their Application in Vanadium Flow Battery. *J. Power Sources* **2014**, *247*, 629–635.

(34) Dai, W.; Shen, Y.; Li, Z.; Yu, L.; Xi, J.; Qiu, X. SPEEK/Graphene Oxide Nanocomposite Membranes with Superior Cyclability for Highly Efficient Vanadium Redox Flow Battery. *J. Mater. Chem. A* **2014**, *2*, 12423–12432.

(35) Hickner, M. A.; Ghassemi, H.; Kim, Y. S.; Einsla, B. R.; McGrath, J. E. Alternative Polymer Systems for Proton Exchange Membranes (PEMs). *Chem. Rev.* **2004**, *104*, 4587–4612.

(36) Swier, S.; Ramani, V.; Fenton, J. M.; Kunz, H. R.; Shaw, M. T.; Weiss, R. A. Polymer Blends Based on Sulfonated Poly(Ether Ketone) and Poly(Ether Sulfone) as Proton Exchange Membranes for Fuel Cells. *J. Membr. Sci.* **2005**, *256*, 122–133.

(37) Choe, H. S.; Carroll, B. G.; Pasquariello, D. M.; Abraham, K. M. Characterization of Some Polyacrylonitrile-Based Electrolytes. *Chem. Mater.* **1997**, *9*, 369–379.

(38) Zussman, E.; Yarin, A. L.; Bazilevsky, A. V.; Avrahami, R.; Feldman, M. Electrospun Polyacrylonitrile/Poly(Methyl Methacrylate)-Derived Turbostratic Carbon Micro-/Nanotubes. *Adv. Mater.* **2006**, *18*, 348–353.

(39) Tran, C.; Kalra, V. Co-continuous Nanoscale Assembly of Nafion-Polyacrylonitrile Blends within Nanofibers: A Facile Route to Fabrication of Porous Nanofibers. *Soft Matter* **2013**, *9*, 846–852.

(40) Kerres, J. A. Blended and Cross-linked Ionomer Membranes for Application in Membrane Fuel Cells. *Fuel Cells* **2005**, *5*, 230–247.

(41) Kerres, J. Covalent-Ionically Cross-linked Poly-(Etheretherketone)-Basic Polysulfone Blend Ionomer Membranes. *Fuel Cells* **2006**, *6*, 251–260.

(42) Li, Z.; Dai, W.; Yu, L.; Xi, J.; Qiu, X.; Chen, L. Sulfonated Poly(Ether Ether Ketone)/Mesoporous Silica Hybrid Membrane for High Performance Vanadium Redox Flow Battery. *J. Power Sources* **2014**, *257*, 221–229.

(43) Mohammadi, T.; Skyllas-Kazacos, M. Evaluation of the Chemical Stability of Some Membranes in Vanadium Solution. *J. Appl. Electrochem.* **1997**, *27*, 153–160.

(44) Sukkar, T.; Skyllas-Kazacos, M. Membrane Stability Studies for Vanadium Redox Cell Applications. *J. Appl. Electrochem.* **2004**, *34*, 137–145.

(45) Winardi, S.; Raghu, S. C.; Oo, M. O.; Yan, Q.; Wai, N.; Lim, T. M.; Skyllas-Kazacos, M. Sulfonated Poly (Ether Ether Ketone)-Based Proton Exchange Membranes for Vanadium Redox Battery Applications. *J. Membr. Sci.* **2014**, *450*, 313–322.

(46) Inan, T. Y.; Dogan, H.; Unveren, E. E.; Eker, E. Sulfonated PEEK and Fluorinated Polymer Based Blends for Fuel Cell Applications: Investigation of the Effect of Type and Molecular Weight of the Fluorinated Polymers on the Membrane's Properties. *Int. J. Hydrogen Energy* **2010**, *35*, 12038–12053.

(47) Wang, J.; Yue, Z.; Economy, J. Preparation of Proton-Conducting Composite Membranes from Sulfonated Poly(Ether Ether Ketone) and Polyacrylonitrile. *J. Membr. Sci.* **2007**, *291*, 210–219.

(48) Wu, Q.; Chen, X.; Wan, L.; Xu, Z. Interactions between Polyacrylonitrile and Solvents: Density Functional Theory Study and Two-Dimensional Infrared Correlation Analysis. *J. Phys. Chem. B* **2012**, *116*, 8321–8330.

(49) Kreuer, K. D. On the Development of Proton Conducting Polymer Membranes for Hydrogen and Methanol Fuel Cells. *J. Membr. Sci.* **2001**, *185*, 29–39.

(50) Mauritz, K. A.; Moore, R. B. State of Understanding of Nafion. *Chem. Rev.* **2004**, *104*, 4535–4585.

(51) Kreuer, K. D. Ion Conducting Membranes for Fuel Cells and other Electrochemical Devices. *Chem. Mater.* **2014**, *26*, 361–380.